Available online at www.sciencedirect.com
ScienceDirect
Journal of Nuclear Materials 373 (2008) 75–81
journal of nuclear materials
www.elsevier.com/locate/jnucmat

Release of gases from uranium metal at high temperatures

Y.S. Sayi [a,*], P.S. Ramanjaneyulu [a], C.S. Yadav [a], P.S. Shankaran [a], G.C. Chhapru [a], K.L. Ramakumar [a], V. Venugopal [b]

[a] *Radioanalytical Chemistry Section, Bhabha Atomic Research Centre, Mumbai 400 085, India*
[b] *Radiochemistry and Isotope Group, Bhabha Atomic Research Centre, Mumbai 400 085, India*

Received 13 November 2006; accepted 30 April 2007

Abstract

Depending on the ambient environmental conditions, different gaseous species could get entrapped in uranium metal ingots or pellets. On heating, melting or vapourising uranium metal, these get released and depending on the composition, may cause detrimental effects either within the metal matrix itself or on the surrounding materials/environment. For instance, these gases may affect the performance of the uranium metal, which is used as fuel in the heavy water moderated research reactors, CIRUS and DHRUVA. Hence, detailed investigations have been carried out on the release of gases over a temperature range 875–1500 K employing hot vacuum extraction technique, in specimen uranium pellets made from uranium rods/ingots. Employing an on-line quadrupole mass spectrometer, the analysis of released gases was carried out. The isobaric interference between carbon monoxide and nitrogen at $m/e = 28$ in the mass spectrometric analysis has been resolved by considering their fragmentation patterns. Since no standards are available to evaluate the results, only the reproducibility is tested. The precision (relative standard deviation at 3σ level) of the method is $\pm 5\%$. The minimum detectable gas content employing the method is 5.00×10^{-09} m^3. About 4×10^{-04} m^3/kg of gas is released from uranium pellets, with hydrogen as the main constituent. The gas content increases with storage in air.

PACS: 81.05.Bx; 81.70.Jb; 82.30.Lp

1. Introduction

Uranium is an important nuclear fuel material. In the earliest reactors, natural uranium metal was used as the fuel and aluminum as clad. These reactors were designed to produce plutonium. Aluminum was chosen as clad due to its low thermal neutron absorption cross-section and high corrosion resistance. However, due to low melting temperature, it was not used in power reactors. To overcome the problems encountered with aluminum, Mg–Al and Mg–Al–Zr alloys were chosen. Uranium (natural and depleted) is used as fuel in the gas cooled reactors, gas cooled fast reactors and lead cooled reactors. The gas cooled fast reactors with helium as coolant and liquid metal (Pb or Pb–Bi) cooled reactors are suitable both for power generation and for thermochemical hydrogen production. Uranium in alloy form is also employed as fuel in nuclear submarines. The accelerator driven reactor systems also use uranium as fuel. In light water reactors (LWR), enriched uranium as UO_2 is used.

Uranium metal is produced by different methodologies [1–4]. Based on the expected burn-up aimed at, the fissile atom density has to be increased. This is generally achieved by employing enriched uranium. There are several methods available for the enrichment of uranium. LASER technique is one of the most sensitive and economical methodologies. However, it is in the developing stages in several countries. LASER method employs either molecular or atomic approach, the later judged as better one. In Atomic Vapour Laser Isotope Separation (AVLIS) technique, uranium vapour, produced by heating uranium metal to ~2500 K, is subjected to selective ionisation followed by magnetic

* Corresponding author. Tel.: +91 22 25595011; fax: +91 22 25505150/1/2.
E-mail address: yssayi@barc.gov.in (Y.S. Sayi).

0022-3115/$ - see front matter © 2007 Elsevier B.V. All rights reserved.
doi:10.1016/j.jnucmat.2007.04.053

sector separation [5]. Uranium is also a starting material for the fabrication of several alloys, which are employed as fuels in different reactors.

The uranium metal rods/ingots fabricated will be left with a few non metallic impurities like hydrogen, nitrogen, oxygen and carbon [6], in either free or combined form. The free gaseous impurities will be present as occluded gases trapped in the interstitial spaces of the metal matrix. During heating of the metal, the occluded gases will be released. At higher temperatures, UH and UN will decompose to give H_2 and N_2, and $[UO]_U$ reacts with $[UC]_U$ to form CO_2 and/or CO depending on the temperature [7]. All these gaseous products will cause pressure build-up in the hermetically sealed fuel pin. In the AVLIS technique of enrichment, adequate uranium vapour pressure (~10 Pa) is to be maintained. In the actual practice, large quantities of uranium metal are heated to ~2500 K, under vacuum to achieve the required vapour pressure of uranium. The gases released from uranium metal deteriorate the efficiency of furnace and the pumping system wherein the evaporation of uranium is taking place.

In the nuclear reactors, the temperature to which the fuel reaches, is dictated by the operating conditions of the reactor, the clad, the coolant and the thermal conductivity of the fuel, while in AVLIS it is heated to ~2500 K. Thus it is seen that, uranium gets heated to different temperatures, depending on the application.

It is, therefore, essential to have a knowledge of the total amount and the composition of gases released from uranium, at different temperatures. With this in view, exhaustive studies have been carried out, over a temperature range 873–1500 K, employing hot vacuum extraction followed by quadrupole mass spectrometry. The upper limit of temperature is chosen so as to carry out the experiments up to near melting temperature of uranium metal. The present paper deals in detail about the temperature calibration of the system and computation of the composition and the concentration of released gases, from the mass spectral data, the fragmentation coefficients and the respective relative sensitivity factors.

2. Experimental

2.1. Equipment

Leybold Heraeus, total gas analyser Model VH-9S has been employed in all the experiments. Schematic diagram of the system is shown in Fig. 1. Total gas analyser is essentially a static ultra high vacuum system. Since the amount of total gas content is very small, the equipment should hold the vacuum under static conditions for several hours. Detailed description of the equipment is given elsewhere [7].

Optical pyrometer (PYRO micro optical pyrometer, USA) and Dataquad DXM quadrupole mass spectrometer, UK were employed for measuring the temperature and composition, respectively.

2.2. Procedure

2.2.1. Sample preparation

Two batches of uranium samples (a) 10 mm long, 3 mm dia and weighing about 3.0 g each and (b) 5 mm long, 3 mm dia and weighing about 1.5 g were taken from same lot of uranium rod. To minimize the contamination of the system and the tungsten crucible with uranium vapour and with molten uranium, uranium metal aliquot is taken in double containment. The sample is taken in tantalum cup and is closed with a lid having 1 mm circular hole. This is enclosed in another tantalum crucible. The above setup is loaded in the tungsten crucible and covered with tungsten lid having three 1 mm dia circular holes. The crucible arrangement is shown in Fig. 2. The vapour pressure of uranium is low (3.95×10^{-7} Pa at 1500 K). Since the holes in the lids (tantalum lid and tungsten lid) are not in same line, most of the uranium vapour will hit the container or the lid and the possibility of the vapour coming out, is reduced. In the experiments carried out above the melting temperature of uranium, liquid uranium metal will be contained in the tantalum crucible and will not come in direct contact with the tungsten crucible.

2.2.2. Sample loading

The sample taken in the tantalum crucible assembly, is loaded in a tungsten crucible by opening the sample port in a flow of inert gas. The tungsten crucible is closed with a tungsten lid having three 1 mm dia holes. The complete crucible assembly is transported to the heating zone employing vertical, horizontal and angular vacuum manipulators. The system is evacuated and degassed at room temperature for 2–3 h at 10^{-3} Pa.

2.2.3. Gas extraction

The sample is heated to the required temperature and time by induction heating. The temperature is measured by optical pyrometer. The gases released are extracted employing mercury ejector pump, into a pre-calibrated volume through a refrigerated cold trap (to remove condensable gases). For the absolute and accurate measurement of the pressure exerted, a McLeod gauge is used. Small amount of this gas is then fed into the electron impact ion source of on-line quadrupole mass spectrometer, through a micro leak valve and several spectra are scanned.

2.2.4. Temperature calibration

Heating of the sample (contained in tungsten crucible) is carried out by water cooled induction heating of 330 kHz frequency. The temperature is varied by suitably selecting the anode current and anode voltages of the induction coil, using power regulation potentiometer. A disappearing filament type optical pyrometer is employed to measure the temperature. To achieve the black body conditions, to the maximum possible extent, the tungsten crucible is covered with a tungsten lid having three 1 mm dia holes, and the optical pyrometer is focused through one of the

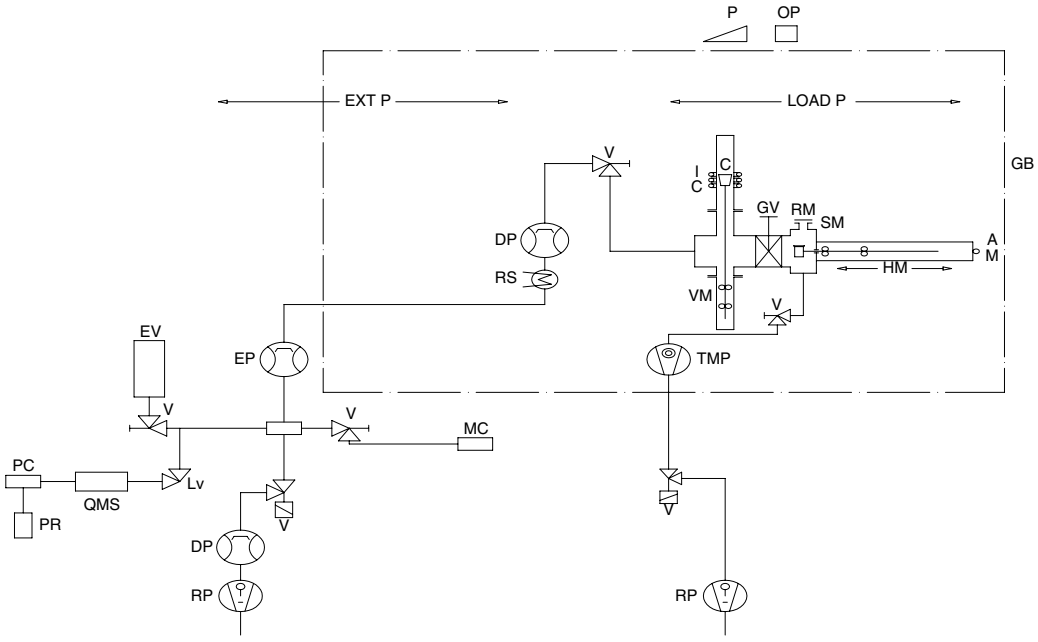

Fig. 1. Total gas analyser system. Load P: sample loading part, extn. P: gas extraction part, SP: sample port, HM/AM/VM/RM: horizontal/angular/vertical/rotational vacuum manipulator; GV: gate valve; C: tungsten crucible; IC: induction coil; DP: mercury diffusion pump; EP: mercury ejector pump; TMP: turbomolecular pump; RP: rotary pump; V: valve; LV: leak valve; MC: McLeod gauge; EV: extra volume; RS: refrigeration system; QMS: quadrupole mass spectrometer; P: prism, OP: optical pyrometer; PC: personal computer; PR: printer; GB: glove box.

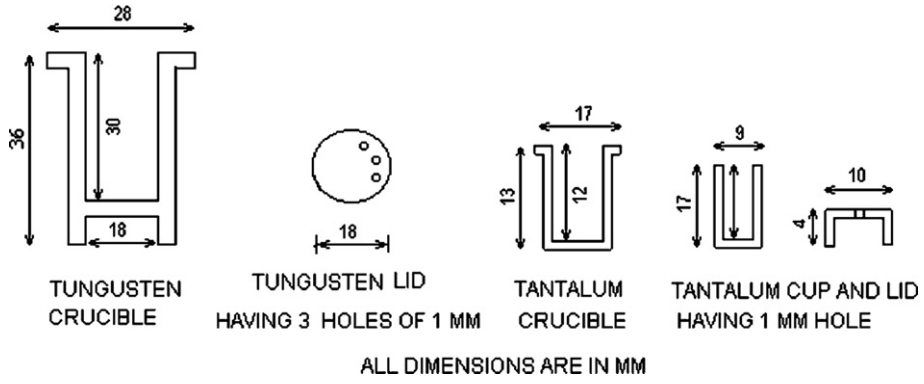

Fig. 2. Crucible arrangement.

holes. In the present studies, the intensity of the tungsten filament, whose intensity can be varied, is matched with the brightness of the object. The current applied to the tungsten filament is a measure of the temperature. The intensity of the object is viewed through a right angle prism and two quartz windows. The emitted radiation from the object, therefore, passes through all these barriers via vacuum and air. Hence it is necessary to incorporate the corrections to the apparent temperature (measured) to obtain the actual temperature. The true temperature is derived from the equation [8].

$$1/T_{\text{true}} - 1/T_{\text{apparent}} = C, \tag{1}$$

where C is a constant. C can be obtained from T_{apparent} measured for known melting point materials (T_{true}). Gold (1336 K), CeF_3 (1773 K) and Pt (2042 K) were chosen and the T_{apparent} was determined by incipient melting temperature technique under similar experimental conditions, i.e., heating the sample at a particular potentiometer setting, quenching and physical examination for the melting or globule formation. From the T_{true} and T_{apparent} values, C has been determined for the present system. The correction factor was incorporated in all other temperatures measured to obtain true temperatures. A linear plot was constructed between the T_{true} and the potentiometer reading (Fig. 3) over the temperature range 1200–2200 K. The linear calibration plot so obtained was extrapolated to below the experimental points. Since the optical pyrometer can be best used above 1200 K, lower temperatures were read from this extrapolated plot. The validity of the extrapolation was tested by measuring the melting temperatures of sodium chloride salt (1073 K) and aluminum (931 K)

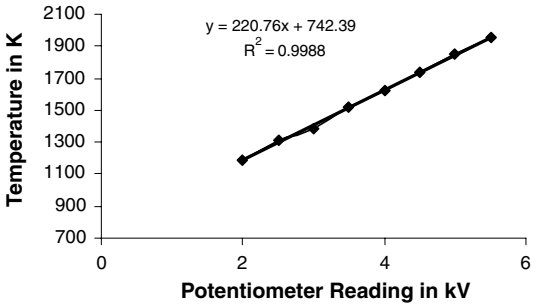

Fig. 3. Temperature calibration.

as a function of potentiometer settings. The temperatures agreed well within ±25 K.

2.2.5. Gas content

The system is made static and the sample is heated at 873 K. The released gas is extracted for 40 min. The pressure is monitored at regular intervals of time. The gas is fed to the quadrupole mass analyser and the mass spectra were recorded, for the determination of gas composition. The gas is then pumped out and the procedure is repeated at next higher temperature. At all these temperatures and time intervals, the blank is also recorded. From the volume of the system and the pressure exerted by the occluded gases, after making the correction for the blank, the total gas content is calculated employing ideal gas equation

$$P_1V_1/T_1 = P_2V_2/T_2, \quad (2)$$

where P_1 = corrected pressure in atmosphere (1.013×10^{05} Pa) exerted by the released gas; V_1 = volume of the system into which the gas is collected; T_1 = room temperature in K; P_2 = atmospheric pressure i.e., 1 atm (1.013×10^{05} Pa); $T_2 = 273$ K and V_2 = the gas content at STP conditions. From this gas content per gram of the sample is calculated.

The accuracy of the method is therefore reflected from the errors in measuring the volume, pressure and weight. The volume of the system is calculated by expanding known amount of dry nitrogen in to the system and measuring the pressure changes for 20 times. It was found to be 16.14 ± 0.10 l and is fixed in all the subsequent measurements. The relative error in the measurement of pressure employing McLeod gauge is 0.95% as given by the McLeod fabricators. For each experiment 1–3 g of sample is weighed in an analytical balance that can read up to 0.0001 g. From these individual errors, the cumulative error calculated based on error propagation comes to 3% (at 3σ level/99% confidence level). The detection limit for the system is 5.00×10^{-9} m^3 at STP.

2.2.6. Gas composition

For the determination of the gas composition, after measuring the pressure, small amount of the gas is fed to the on-line quadrupole mass spectrometer through a micro leak valve. The quadrupole mass analyser has 90 mm long quadrupole having a resolution of $M/\Delta M \geqslant M$ at 10% valley height. The resolution of the quadrupole mass spectrometer is determined by taking an equimolar ^{20}Ne and ^{22}Ne. It is found to be 45 at m/e 20. Ions are produced by an electron bombardment source with a thoria coated iridium filament having an electron energy of 80 eV. The mass range of the system is 1–100 amu. The ion currents are measured employing a Faraday cup detector. The peak intensities at m/e 2 (H_2^+), 12 (C^+), 14 (N^+/CH_2^+), 15 (CH_3^+), 16 (O^+/CH_4^+), 28 (N_2^+/CO^+), 32 (O_2^+) and 44 (CO_2^+) are recorded.

3. Results and discussion

3.1. Time of heating

The data of the gas content released at different temperatures, as a function of time, is presented in Fig. 4. It can be seen from the figure that all the gases are released at all the temperatures measured, well within 20 min, and hence the subsequent measurements were confined to 30 min of heating.

3.2. Cumulative yields of gases

The gas content is determined starting from the lowest temperature. After measuring the gas content and the determining its composition, the gas is completely evacuated to 10^{-03} Pa. The system is made static and the temperature is raised to the next desired value and measurements are carried out. The procedure is repeated until the highest temperature is attained. The cumulative gas content is obtained by addition of the data from lowest temperature to that temperature.

3.3. Gas composition

The gas composition is calculated from the peak intensities (ion current) at various m/e ratios after correcting for blank spectra. It is well-established fact that poly-atomic gases undergo fragmentation in addition to ionisation when bombarded with electrons of energy ~80 eV [9]. This fragmentation pattern could be used to resolve the gases like carbon monoxide and nitrogen. The ion current (peak

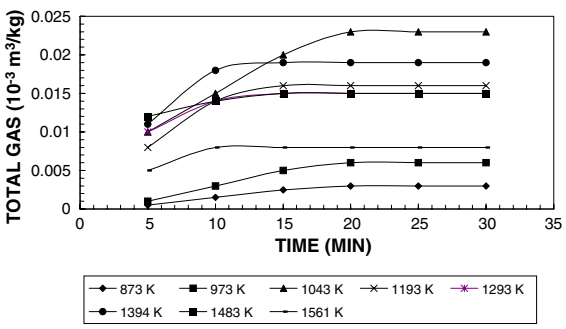

Fig. 4. Time vs. gas content at different temperature.

intensity or sensitivity) also depends on the nature of gas. It is therefore essential to apply the necessary corrections to evaluate the partial pressures from mass spectral data. To arrive at the fragmentation patterns and the sensitivity factors, pure gases are taken into a chamber at 1–2 Pa. This gas is injected into the mass analyser through a micro leak valve at $2–8 \times 10^{-3}$ Pa. Peak intensities are recorded. The percentage of pattern coefficients obtained as the ratios of various fragmentation peak intensities in pure gases are constant (well within 5%), over the working pressure range, indicating that these coefficients are independent of pressure under the experimental conditions. The *m/e* of the fragments and their percentages for the different gases as determined by feeding pure gases are given below:

Methane: C^+ (12, 1%), CH^+ (13, 3%), CH_2^+ (14, 9%), CH_3^+ (15, 40%) and CH_4^+ (16, 47%)
Nitrogen: N^+/N_2^{2+} (14, 6%) and N_2^+ (28, 94%)
Carbon monoxide: C^+ (12, 4%), O^+ (16, 1%) and CO^+ (28, 95%)
Carbon dioxide: C^+ (12, 5%), O^+ (16, 6%), CO^+ (28, 9%) and CO_2^+ (44, 80%)

In obtaining the percentage of fragmentation coefficients of above gases, only the most abundant isotopes of the elements are considered. The values agreed well with data provided by Dataquad Quadrupole Mass Spectrometer of Anglo Scientific Instruments, UK and the literature values [9].

It can be seen from the above data that peak at *m/e* 15 and 44 are specific only for methane and carbon dioxide, respectively. In our earlier studies [10] it is seen that the oxides of nitrogen, viz., NO, N_2O and NO_2 will invariably show peak at *m/e* 30. In sample spectra, absence of peak at *m/e* 30 indicates their absence and hence peak at *m/e* 44 is due to carbon dioxide only. From the peak height at *m/e* 44, the contribution at 12 ($p_{12(CO_2)}$) and 28 ($p_{28(CO_2)}$) due to carbon dioxide are calculated from the fragmentation coefficients. Similarly, contribution at 12 ($p_{12(CH_4)}$) and 16 ($p_{16(CH_4)}$) due to methane are calculated from the peak intensity at 15. The difference between the peak intensity ($p_{12(obs)} - p_{12(CO_2)} - (p_{12(CH_4)})$) gives $p_{12(CO)}$, a measure of carbon monoxide. From $p_{12(CO)}$ peak intensity, contribution of carbon monoxide at peak 28 $p_{28(CO)}$ is calculated. Nitrogen contribution at peak 28 ($p_{28(N_2)}$) is calculated as ($p_{28(obs)} - p_{28(CO_2)} - p_{28(CO)}$). Thus, we obtain the peak intensities at the parent peaks of methane (16), carbon monoxide (28), nitrogen (28) and carbon dioxide (44). The ion current (peak intensity) also depends on the type of gas. Therefore, these intensities need to be further corrected for sensitivity factors. These sensitivity factors depend on the energy of the electron current and the ionisation cross sections [11–13]. Generally, these sensitivity factors are normalised with respect to nitrogen, whose sensitivity factor is taken as unity.

From the mass spectral data recorded for various pure gases, H_2, N_2, CH_4, CO and CO_2, the peak intensities at nearly same pressures in the mass analyser were selected and the corresponding parent peak intensities were calculated. The ratios of the parent peak intensities of the gases with respect to nitrogen were calculated and are taken as relative sensitivity factors (RSF). The reciprocal of the RSF are taken as correction factors (CF). The correction factors were $N_2 = 1$; $H_2 = 2.45$, $CH_4 = 0.8$, $CO = 0.92$; $CO_2 = 0.69$. These experimental correction factors were comparable with the theoretical values (±10%) obtained from the ionisation cross sections at 80 eV [11–13]. Further, to validate the correction factors in gas mixtures, binary mixtures of N_2 with CO and H_2 over a range of 5–95% were prepared and gas composition was determined by QMS by feeding the gas into the mass analyser, through micro leak valve. The composition was also determined in these mixtures by gas chromatography. Results obtained by both the methods were in good agreement indicating that the correction factors hold good even in the gaseous mixtures [14].

From the mass spectral data and the fragmentation patterns, the peak intensities of the gases present in the released gases are calculated. It is multiplied with the corresponding correction factor (CF) to obtain its corrected peak intensity ((peak intensity)$_i$). Since the peak intensity is directly proportional to its partial pressure, the composition of the species (*i*) is given as

$$P_i = P_t(\text{peak intensity})_i \Big/ \sum(\text{peak intensity})_i, \quad (3)$$

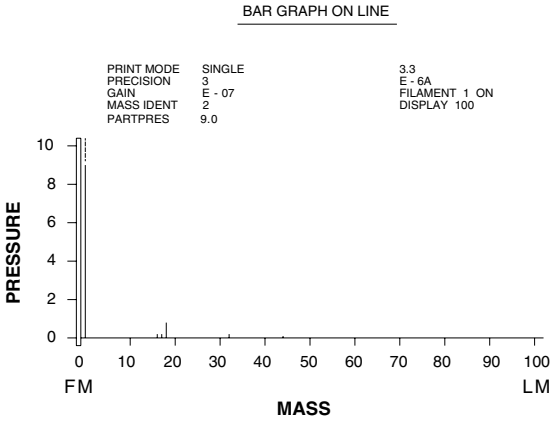

Fig. 5. Typical mass spectra.

Table 1
Peak intensities

Mass	Typical spectra peak intensities (amp/Pa)	
	Blank	Sample (after correcting for blank)
2	1.4×10^{-6}	8.0×10^{-5}
12	6.0×10^{-8}	1.2×10^{-6}
14	8.0×10^{-8}	1.0×10^{-6}
15	1.2×10^{-8}	3.0×10^{-6}
28	3.3×10^{-5}	5.0×10^{-5}
32	8.1×10^{-6}	–
44	4.3×10^{-7}	1.4×10^{-5}

Table 2
Total gas content, its composition and concentration in uranium metal

Sample no. and heating information	Temperature[a] (K)	Gas content (m^3/kg)		Cumulative (m^3/kg)					Cumulative concentration (mg/kg)				
		m^3/kg	Cumulative	H_2	N_2	CO	CO_2	CH_4	H_2	N_2	CO	CO_2	CH_4
Sample no. 1 step wise heating	853	1.50×10^{-5}	1.50×10^{-5}	1.20×10^{-5}	0.20×10^{-5}	0.05×10^{-5}	0.06×10^{-5}	0.02×10^{-5}	1.07	3.00	0.60	1.15	0.12
	908	6.10×10^{-5}	7.70×10^{-5}	7.10×10^{-5}	0.30×10^{-5}	0.15×10^{-5}	0.11×10^{-5}	0.11×10^{-5}	6.35	3.38	1.83	2.13	0.77
	1018	6.90×10^{-5}	1.46×10^{-4}	1.37×10^{-4}	0.40×10^{-5}	0.16×10^{-5}	0.12×10^{-5}	0.13×10^{-5}	12.30	5.49	1.96	2.29	0.91
	1123	8.00×10^{-5}	2.26×10^{-4}	2.15×10^{-4}	0.50×10^{-5}	0.19×10^{-5}	0.12×10^{-5}	0.13×10^{-5}	19.40	5.74	2.31	2.36	0.95
	1233	8.50×10^{-5}	3.11×10^{-4}	2.99×10^{-4}	0.50×10^{-5}	0.19×10^{-5}	0.12×10^{-5}	0.13×10^{-5}	26.90	6.87	2.31	2.36	0.96
	1343	4.70×10^{-5}	3.58×10^{-4}	3.48×10^{-4}	0.50×10^{-5}	0.19×10^{-5}	0.12×10^{-5}	0.15×10^{-5}	31.33	6.87	2.31	2.36	1.04
	1448[b]	2.50×10^{-5}	3.83×10^{-4}	3.75×10^{-4}	0.50×10^{-5}	0.19×10^{-5}	0.12×10^{-5}	0.16×10^{-5}	33.70	6.87	2.31	2.36	1.16
Sample no. 2 direct heating	1448[b]	3.64×10^{-4}	3.64×10^{-4}	3.57×10^{-4}	0.40×10^{-5}	0.10×10^{-5}	–	0.20×10^{-5}	32.13	5.00	1.24	0.00	1.11
Sample no. 3 direct heating	1498[b]	3.80×10^{-4}	3.80×10^{-4}	3.74×10^{-4}	0.30×10^{-5}	0.10×10^{-5}	0.02×10^{-5}	0.20×10^{-5}	33.66	3.75	1.39	0.32	1.46
Sample no. 4 direct heating	1448[b,c]	2.08×10^{-4}	2.08×10^{-4}	1.95×10^{-4}	0.50×10^{-5}	0.50×10^{-5}	0.11×10^{-5}	0.20×10^{-5}	17.55	6.25	5.78	2.21	1.29
Sample no. 5 direct heating	1498[b,c]	2.17×10^{-4}	2.17×10^{-4}	2.09×10^{-4}	0.30×10^{-5}	0.30×10^{-5}	0.06×10^{-5}	0.10×10^{-5}	18.81	3.75	3.18	1.27	0.95

[a] Duration of heating is 30 min.
[b] Uranium melted.
[c] Samples are stored in desiccator.

where P_t is the total pressure and P_i is the partial pressure of the species i. A typical mass spectrum of the gases released, in bar graph mode, is given in Fig. 5. Typical data of the blank, gases released from typical uranium pellets (after incorporating the correction for the blank) are given in Table 1. From the partial pressures and the total pressures, the gas composition and the concentration in mg/kg of U (ppmw) was calculated using ideal gas laws. The results are shown in the Table 2. The pictorial representation of the various gases released over a temperature range 873–1500 K is given in Fig. 6.

The gases released during heating of uranium is a mixture of the occluded gases and the reaction product of the impurities present in it. The gaseous products are formed as under:

$$[UO]_U + [UC]_U \rightarrow U + (CO) \quad (4)$$

$$[UO]_U + [UC]_U \rightarrow U + (CO_2) \quad (5)$$

$$[UN]_U \rightarrow U + (N_2) \quad (6)$$

$$[UH]_U \rightarrow U + (H_2) \quad (7)$$

$$[UH]_U + [UC]_U \rightarrow U + (CH4) \quad (8)$$

From Table 2, it can be seen that when the samples is heated directly to a temperature 1448 K and above, the CO_2 content is less than the one obtained in the step wise heating. This is due to the less stability of CO_2 at higher temperatures and CO formation is more favorable. Formation and release of methane is significant up to 1000 K. Above this temperature, since methane is not stable, it may be decomposing into hydrogen and carbon. It can be observed from Table 2, that the release of hydrogen content increases with temperature. At lower temperatures, the occluded hydrogen is released. With increase in temperature, decomposition of UH takes place and contributes to the hydrogen content. The process continues till the entire amount of UH decomposes. It can be seen from Fig. 6, that the entire amount hydrogen in whatever form it is present, gets released completely by 1400 K. Considering the uncertainties in determination of fragmentation patterns and correction factors, the error in determination of composition of gas could be ±10%.

Since uranium nitride is more stable, it will not decompose even at 1500 K. The concentration of nitrogen

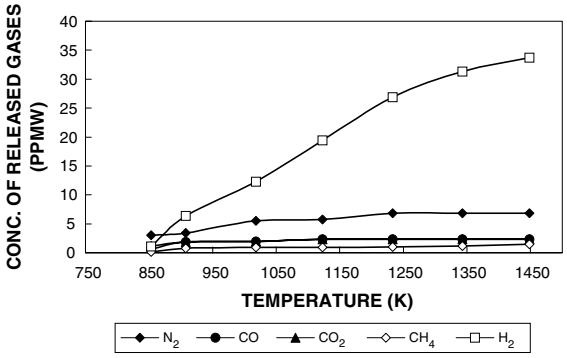

Fig. 6. Temperature vs. gas composition.

obtained up to this temperature is the nitrogen content, present as occluded gas in the interstitial spaces. At higher temperatures, above 1800 K, UN starts decomposing and it also contributes to the gases released. In AVLIS technique of enrichment of uranium, the metal will be heated above 2500 K. At this temperature UN decomposes and N_2 will also be liberated. Hence, total nitrogen content plays an important role for amount of gas released in enrichment process.

The small variation in the gas content in all these experiments is due the fact that these samples were analysed at different time intervals.

For finding out the effect of storing, the pellets were stored in air atmosphere and in a desiccator. The gas content was analysed. Gas content at 1448 and 1498 K were found to be 3.60×10^{-04} m^3/kg and 2.00×10^{-04} m^3/kg, respectively for air and desiccator stored ones. This indicates that the pick up is more in the air stored pellets.

4. Conclusion

The amount of gases released from uranium pellet is about 4.00×10^{-04} m^3/kg. Gas composition is determined from mass spectral data by considering the fragmentation pattern and correction factors. Hydrogen content is more than 90% when the pellet is heated to ~1450 K. Above 2000 K, nitrogen pressure also may increase due to the decomposition of UN. The environmental conditions will play an important role in the pick up of gas by the uranium metal necessitating adopting strict storage conditions.

References

[1] E. Peligot, J. Prakt. Chem. 1 (1841) 442.
[2] H.A. Wilhelm, Met. Prog. 69 (1956) 81.
[3] T. Suzuki, T. Sakata, H. Tsuchiya, K. Ota, Y. Takasawa, N. Teramae, S. Yamagami, K. Endo, Proc. Electrochem. Soc. 96 (1996) 204.
[4] H. Moissan, Compt. Rend. 116 (1893) 347.
[5] P. Ramakoteswara Rao, Curr. Sci. 85 (2003) 615.
[6] Y.S. Sayi, C.S. Yadav, P.S. Shankaran, G.C. Chhapru, K.L. Ramakumar, V. Venugopal, Met. Mater. Process. 14 (2002) 319.
[7] Y.S. Sayi, C.S. Yadav, P.S. Shankaran, G.C. Chhapru, Indian J. Chem. Technol. 11 (2004) 648.
[8] W.P. Wood, J.M. Cork, Pyrometry, Mc-Graw-Hill Book Co., Inc., 1941.
[9] A. Breth, R. Dobrozemsky, B. Kraus, Vaccum 33 (1983) 73.
[10] Y.S. Sayi, C.S. Yadav, P.S. Shankaran, G.C. Chhapru, K.L. Ramakumar, V. Venugopal, Int. J. Mass Spectrom. 214 (2002) 375.
[11] H.C. Straub, P. Renault, B.G. Lindsay, K.A. Smith, R.F. Stebbings, Phys. Rev. A 54 (1996) 2146.
[12] H.C. Straub, B.G. Lindsay, K.A. Smith, R.F. Stebbings, J. Chem. Phys. 105 (1996) 4015.
[13] M.A. Mangan, B.G. Lindsay, R.F. Stebbings, J. Phys. B: At. Mol. Opt. 33 (2000) 3225.
[14] Y.S. Sayi, J. Radhakrishna, C.S. Yadav, P.S. Shankaran, G.C. Chhapru, Anal. Lett. 23 (1990) 2049.